Iranian Journal of Oil & Gas Science and Technology, Vol. 7 (2018), No. 1, pp. 40-59
http://ijogst.put.ac.ir

Integrated Characterization and a Tuning Strategy for the PVT Analysis of Representative Fluids in a Gas Condensate Reservoir

Shahriar Osfouri[1*], Reza Azin[2], Hamid Reza Amiri[3], Zahra Rezaei[4], and Mahmoud Moshfeghian[5]

[1] Associate Professor, Department of Chemical Engineering, Faculty of Petroleum, Gas, and Petrochemical Engineering, Persian Gulf University, Bushehr, Iran
[2] Associate Professor, Department of Petroleum Engineering, Faculty of Petroleum, Gas, and Petrochemical Engineering, Persian Gulf University, Bushehr, Iran
[3] M.S. Student, Department of Petroleum Engineering, Faculty of Petroleum, Gas, and Petrochemical Engineering, Persian Gulf University, Bushehr, Iran
[4] M.S. Student, Department of Chemical Engineering, Faculty of Petroleum, Gas, and Petrochemical Engineering, Persian Gulf University, Bushehr, Iran
[5] Professor, School of Chemical and Petroleum Engineering, Shiraz University, Shiraz, Iran

Received: February 16, 2017; *revised*: June 26, 2017; *accepted*: July 11, 2017

Abstract

Gas condensate reservoirs are characterized by a distinctive retrograde behavior and potential for condensate drop out during production and sampling. Efficient modeling of gas condensate reservoir requires careful phase behavior studies of samples collected prior to and during the production life of reservoir. In this work, an integrated characterization and tuning algorithm is proposed to analyze the pressure-volume-temperature (PVT) behavior of gas condensate samples. Each characterization and tuning scenario is described by a "path" which specifies the class of fluid, splitting and lumping (if any), the type of correlation, and grouping strategy (static or dynamic). Different characterization approaches were tested for the effective description of heavy end. Meanwhile, dynamic and static strategies were implemented to tune the equation of state (EOS) through non-linear regression. The optimum combination of characterization and tuning approach was explored for each sample by a rigorous analysis of the results. It was found out that the exponential distribution function gives the best performance for heavy end characterization in a dynamic tuning strategy. Also, analyses indicate that using higher single carbon number may not necessarily make EOS tuning more accurate. In addition, the optimum step is reached in either the third or fourth step for most cases in a dynamic tuning approach, and is sensitive neither to the characterization path nor to the selected end carbon number.

Keywords: Gas Condensate, PVT Behavior, Fluid Characterization, EOS Tuning, Plus Fraction

1. Introduction

Gas condensate reservoirs contain hydrocarbon accumulates at a temperature between critical and

* Corresponding Author:
Email: osfouri@pgu.ac.ir

cricondentherm points (Ahmed, 2007). These reservoirs are characterized by a distinctive retrograde behavior and potential to leave beyond heavy ends, known as condensates, in a reservoir during production and sampling (Fevang, 1995; Kool et al., 2001; McCain and Alexander, 1992; Schebetov et al., 2010). The proper and optimized development and modeling of gas condensate reservoirs require careful phase behavior studies of the samples collected prior to and during the production life of reservoir. Reservoir management strategies depend closely on the quality of samples, experiments conducted on them, and the pressure-volume-temperature (PVT) study performed based on these experiments. An integrated approach in sampling, PVT experiment, and phase behavior modeling is essential for a multi-well reservoir to achieve a robust reservoir fluid description. Due to complexities in their phase behavior and flow patterns, the development of gas condensate reservoirs can be associated with several uncertainties. Main PVT analyses for understanding the behavior of gas condensate systems include compositional analysis, constant volume depletion (CVD), and constant composition expansion (CCE) experiments (Ahmed, 1989, 2007; Pedersen et al., 1989; Whitson and Brule, 2000). Phase behavior modeling of hydrocarbon samples, including gas condensates, by using equations of state (EOS) has been a well-known technique applied widely to predicting the PVT behavior of fluid during the production life of a reservoir. These EOS are useful tools for predicting properties such as dew-point pressure, the density of liquid and vapor phases, liquid drop-out across pressure decline, vapor-liquid equilibrium (VLE) calculations etc. (Ahmed, 2007; Imo-Jack, 2010; Nasrifar et al., 2005; Nasrifar and Moshfeghian, 2002; Nazarzadeh and Moshfeghian, 2013; Whitson and Brule, 2000; Yarborough, 1979). Cubic EOS is widely applied to the phase behavior studies of gas condensate systems. A comprehensive classification of EOS are reviewed by Wei and Sadus (Wei and Sadus, 2000). Among the large family of cubic EOS, Peng-Robinson (PR) and Soave-Redlich Kwong (SRK) equations are the two equations of state most familiar to petroleum engineers (Ahmed, 1989, 2007; Nazarzadeh and Moshfeghian, 2013; Peng and Robinson, 1976; Soave, 1972; Whitson and Brule, 2000). Tuning of EOS parameters according to the measured data is a crucial step before applying it to VLE simulations and predicting thermodynamic and physical properties of each phase. Numerous studies have been reported for the tuning strategies of EOS to fit gas condensate data (Aguilar Zurita and McCain, 2002; Danesh, 1998; Hosein and Dawe, 2012; Merrill et al., 1994; Pedersen et al., 1988). Different tuning strategies are described in detail by Whitson (Whitson and Brule, 2000) and Danesh (Danesh, 1998). A tuning strategy coupled with Pedersen splitting method was recently used to tune Patel and Teja EOS (Patel and Teja, 1982) and to study the phase behavior of multiple samples taken from a retrograde gas condensate field (Mehrabian and Crespo, 2011). An important step in EOS modeling is the characterization of heavy end which may cause drastic effects on predictions if not properly conducted. This step involves splitting, lumping, and predicting the physical properties of pseudo-components that provide the best description of heavy end according to reported experimental results (Ahmed, 1989; Danesh, 1998; Whitson, 1983; Whitson and Brule, 2000). Among different techniques employed to characterize plus fraction in gas condensate systems, exponential and gamma distribution functions are most widely used (Al-Meshari et al., 2005; Moshfeghian et al., 2006; Pedersen et al., 1992; Pedersen et al., 1989; Shariati et al., 2001; Whitson et al., 1990). The lumped plus fraction may undergo successive splitting/lumping before EOS can predict dew point pressure within an acceptable range. An integrated characterization and tuning strategy with a focus on EOS parameters will result in a tuned EOS that can predict experimental data within an acceptable range (Danesh, 1998; Whitson and Brule, 2000). This integrated approach has been applied to PVT studies of gas condensate (Al-Meshari et al., 2005; Hosein and Dawe, 2012; Hosein and Jagai, 2003; Merrill et al., 1994) and proved to yield better results.

The objectives of this paper are to present an integrated characterization and tuning algorithm and to apply it to PVT data samples collected from a supergiant multi-well gas condensate reservoir. In the following sections, the properties of the collected samples and measured quantities are presented first. Then, the methodology is proposed and discussed. After that, the proposed methodology is applied to samples, and the results are analyzed to explore the most efficient combination of characterization and tuning procedure for each sample.

2. Experimental data

The experimental data include three representative gas condensate samples which were prepared through screening of more than 80 comprehensive PVT reports collected during 20 years from exploration and production wells in a supergiant, multi-layer, multi-well gas condensate field. The screening criteria considered factors such as quality control of well conditioning, separator, and PVT tests. This was accomplished by using drill-stem test (DST) data and checking stability conditions in the first step, followed by quality checking of PVT data (Osfouri et al., 2014). Also, it was essential to check the quality of separator equilibrium conditions and to validate the consistency of the measured PVT data reported for recombined samples using standard techniques (Thomas et al., 2007; Whitson and Brule, 2000) before EOS tuning. This approach involves comparing the dew point pressure of separator gas with the bubble point pressure of separator liquid samples, using the Hoffman-Standing (Hoffman et al., 1953) plot, comparing condensate-gas ratio (CGR) of the recombined fluid with that of the reservoir fluid, and performing material balance on the measured CVD data. Details of PVT quality control and sampling equilibrium conditions for the samples under study are discussed elsewhere (Osfouri et al., 2014). Although this approach is rather complicated and time consuming, it filters invalid data and focuses on valid data measured in equilibrium conditions for EOS tuning and determining representative fluid(s) in the reservoir. Table 1 summarizes the compositional analysis and plus fraction properties of three representative samples of the studied reservoir.

Table 1

Original composition (mol.%) of gas condensate samples and properties of plus fraction.

Component	Well name		
	W_1	W_2	W_3
N_2	3.26	3.51	3.23
CO_2	1.91	1.92	1.96
H_2S	0.12	0.12	0.15
C_1	82.95	82.79	83.06
C_2	5.33	5.35	5.27
C_3	1.98	2	1.96
i-C_4	0.42	0.43	0.42
n-C_4	0.7	0.72	0.7
i-C_5	0.31	0.32	0.31
n-C_5	0.46	0.29	0.29
C_6	0.49	0.39	0.57
C_7	0.46	0.48	0.47
C_8	0.43	0.45	0.44
C_9	0.28	0.29	0.29
C_{10}	0.21	0.22	0.22
C_{11}	0.15	0.15	0.15

Component	Well name		
	W_1	**W_2**	**W_3**
C_{12+}	0.54	0.57	0.51
Total (mol.)	100	100	100
MW C_{12+}	211.91	214.89	211.25
C_{12+} relative density	0.835	0.837	0.835
Gas MW	22.09	22.12	22.03
Gas relative density	0.763	0.764	0.761

In addition to the analysis given in Table 1, each sample underwent extra compositional analysis with both C_{7+} and C_{20+} as the last heavy components. The wells were drilled in different blocks, and the distribution of hydrocarbon composition within the field may be detected by comparing the PVT data. The experimental data included reservoir fluid compositional analysis, a complete set of constant composition expansion (CCE), and constant volume depletion (CVD) tests along with the separator data for all the samples. According to the experimental data, the dew point pressure of this field was measured in the range of 32.20–34.14 MPa (4682-4950 psia). Tables A1 and A2 in Appendix summarize the measured PVT data used in this study. These data include vapor Z-factor, retrograde liquid relative volume, and cumulative produced moles of liquid drop-out of CVD experiments as well as Z-factor, relative volume, and liquid drop-out of CCE experiments. All the data were used in EOS tuning. Figure 1a shows a typical phase diagram for samples W_1 and W_2, and liquid drop-out versus pressure obtained from CCE test is displayed in Figure 1b; Figure 1C shows Z-factor (obtained from CCE test) versus pressure. According to Figure 1, these representative samples have different phase behaviors although their compositions seem similar as reported in Table 1. Moreover, the PVT reports indicate a 255 psia difference between the measured dew point pressures of these samples.

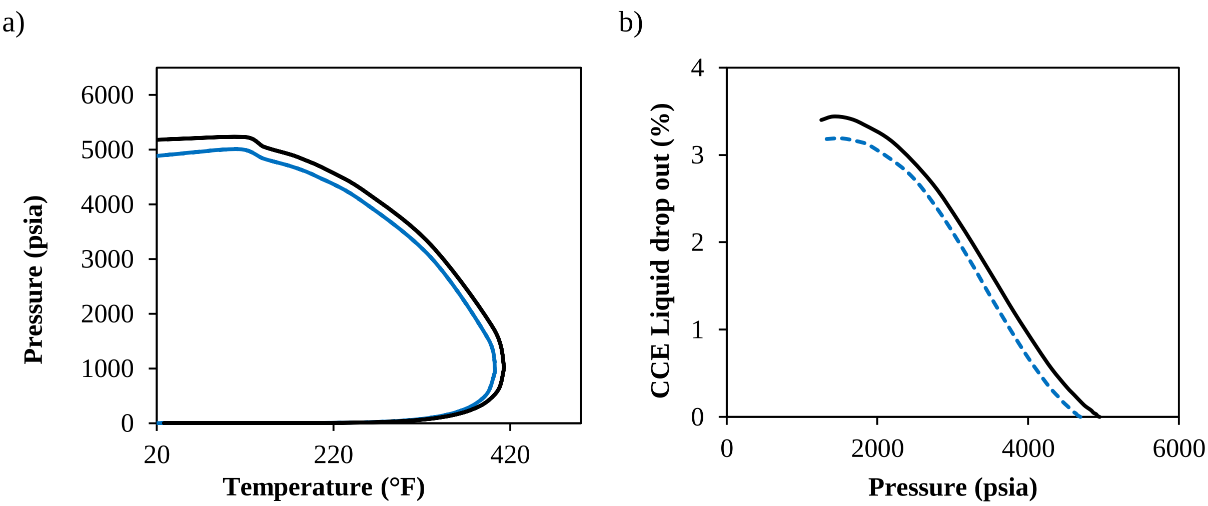

c)

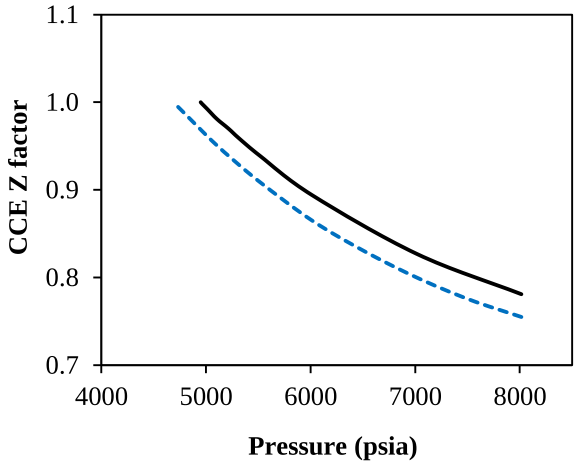

Figure 1
a) P-T diagram, b) liquid drop out, and c) and Z factor of the CCE experiment for representative samples W_1 (solid) and W_2 (dashed).

3. Methodology

In this work, two EOS tuning strategies, named as static and dynamic strategies, were followed to find the best match between the experimental data and EOS predictions using the sum of squares of relative error as the objective function:

$$OF = \sum_i \left(\frac{x_i^{cal} - x_i^{exp}}{x_i^{exp}} \right)^2 \tag{1}$$

where, x_i^{cal} and $x_\mathrm{i}^{\mathrm{exp}}$ are calculated and measured quantities, including dew-point pressure and all the measured properties of CVD and CCE tests. The objective function is minimized using Levenberg-Marquardt algorithm (Edgar, 2001). In both proposed strategies, tuning of EOS is integrated with the characterization of plus fraction. Furthermore, to check the validity of the characterization method, the phase envelope of the samples were checked before and after the characterization of plus fraction. In static tuning, component grouping is fixed and remains unchanged throughout EOS tuning. On the other hand, dynamic tuning involves the modification of component grouping while EOS tuning is in progress. The former strategy focuses on EOS parameters only, while the latter combines EOS tuning with a dynamic component grouping. In this approach, the best distribution function, empirical correlations for estimating critical properties and acentric factor, and lumping procedure are determined in line with optimizing EOS parameters. To this end, the exponential (Pedersen et al. (1989)) and gamma (Whitson et al., 1990) distribution functions were used for describing the pseudo-component single carbon number (SCN) group distributions. In addition, the correlations of Lee-Kesler (Lee and Kesler, 1975) and Twu (Twu, 1984) were used to predict the critical properties and acentric factor of SCN groups. Based on the selected strategy, different combinations of plus fraction splitting (if necessary), component lumping (if necessary), and empirical correlations may be applied for efficient PVT modeling. This will be described as different tuning “paths” as follows. In order to avoid more complexity in EOS modeling, the Peng-Robinson (PR) EOS was used throughout the rest of the study:

$$P = \frac{RT}{v-b} - \frac{\alpha(T)}{v^2 + 2bv - b^2} \tag{2}$$

where,

$$\alpha(T) = [1 + \kappa(1 - \sqrt{T_r})]^2 a_c \tag{3}$$

$$a_c = \Omega_a \frac{R^2 T_c^2}{P_c} \tag{4}$$

$$b = \Omega_b \frac{R T_c}{P_c} \tag{5}$$

and κ is a dimensionless parameter such that:

$$\begin{aligned} &\omega \leq 0.49 \\ &\kappa = 0.37464 + 1.54226\omega - 0.26992\omega^2 \end{aligned} \tag{6}$$

$$\begin{aligned} &\omega > 0.49 \\ &\kappa = 0.379642 \;\; + 1.48503\omega - 0.164423\omega^2 + 0.016666\omega^3 \end{aligned} \tag{7}$$

Ω_a and Ω_b of plus fraction are adjustable parameters of the objective function.

3.1. Static tuning strategy

Based on the available data, three composition classes, named as Class A, Class B, and Class C, were defined, for which characterization and EOS tuning was carried out using the static tuning strategy:

Class A: in this class, the original composition up to C_{12+} was considered in the PVT calculations. Any composition beyond C_{12} was lumped into a C_{12+} pseudo-component, and its critical properties were calculated using empirical correlations. No further grouping was made on the composition. The tuning of EOS was performed by focusing on the critical properties of plus fraction and EOS parameters (Ω_a and Ω_b) for certain components.

Classes B and C: these classes focus on the lumped composition of the samples shown in Tables 2 and 3 respectively. The components used in grouping are different between classes B and C. For class B, the last component was split into C_{12} and C_{13+}, followed by lumping C_{12} with C_7-C_{11} pseudo-components. On the other hand, no splitting was made on the components in class C, and grouping approach was different from that used in class B. Procedures for calculating the critical properties of the lumped components and EOS tuning were similar for all the classes.

Table 2
Composition (mol.%) of the lumped samples (Class B).

Component or group	**W_1**	**W_2**	**W_3**
N_2-C_1	86.21	86.30	86.30
H_2S	0.12	0.12	0.15
CO_2	1.91	1.92	1.96
C_2-C_3	7.31	7.35	7.23
i-C_4 to C_6	2.38	2.15	2.29
C_7 to C_{12}	1.70	1.77	1.73
C_{13+}	0.37	0.39	0.35
Properties of C_{13+}			
MW:	228.92	225.94	225.28
Relative density	0.842	0.843	0.843

Table 3
Composition (mol.%) of the lumped samples (Class C).

Component or group	W_1	W_2	W_3
N_2-C_1	86.21	86.30	86.29
H_2S-CO_2	2.03	2.04	2.11
C_2-C_3	7.31	7.35	7.23
i-C_4 to n-C_5	1.89	1.76	1.72
C_6 to C_8	1.38	1.32	1.48
C_9-C_{11}	0.64	0.66	0.66
C_{12+}	0.54	0.57	0.51
Properties of C_{12+}			
MW:	211.25	219.91	214.89
Relative density	0.835	0.835	0.837

3.2. Dynamic tuning strategy

In this strategy, the single carbon number (SCN) of the plus fraction component is fixed and compared with fluid composition to decide if any further splitting is necessary. If required, splitting will be performed by either exponential or Gamma distribution functions, followed by estimating the critical properties and the acentric factor of the pseudo-components. The calculations are continued through simultaneous component regrouping and EOS tuning by the five-step procedure as described in Whitson (Whitson and Brule, 2000) until the best match between the measured and predicted experiments is obtained. In addition, the phase diagram of the regrouped composition at each stage must be compared with that of the original fluid.

A flow chart and summary of these strategies is shown in Figure 2. In this figure, the dynamic and static strategies are denoted by D and S symbols respectively. Additionally, each strategy is described by a "path" which specifies the class of fluid or the SCN of plus fraction, splitting and lumping (if any), and the type of empirical correlation. For the dynamic strategy, the grouping step is also included. For class B, splitting C_{12+} to C_{12} and C_{13+} was conducted by either exponential (Ex) or Gamma (Ga) distribution functions. For example, the path named as S-B-GA-L refers to a case in the static strategy in which grouping class B with gamma distribution function and Lee-Kesler's (Lee and Kesler, 1975) correlation is studied. The abbreviation "NO" in classes A and C indicates that no splitting was made on them and both are run with composition up to C_{12+}. In the dynamic strategy, for example, D7-EX-L-1 refers to a case in which C_{7+} is split by exponential distribution function, and Lee-Kesler's (Lee and Kesler, 1975) correlation is used to characterize SCN and lumped groups. The last number (1 in this example) refers to the grouping step of Whitson's procedure (Whitson and Brule, 2000).

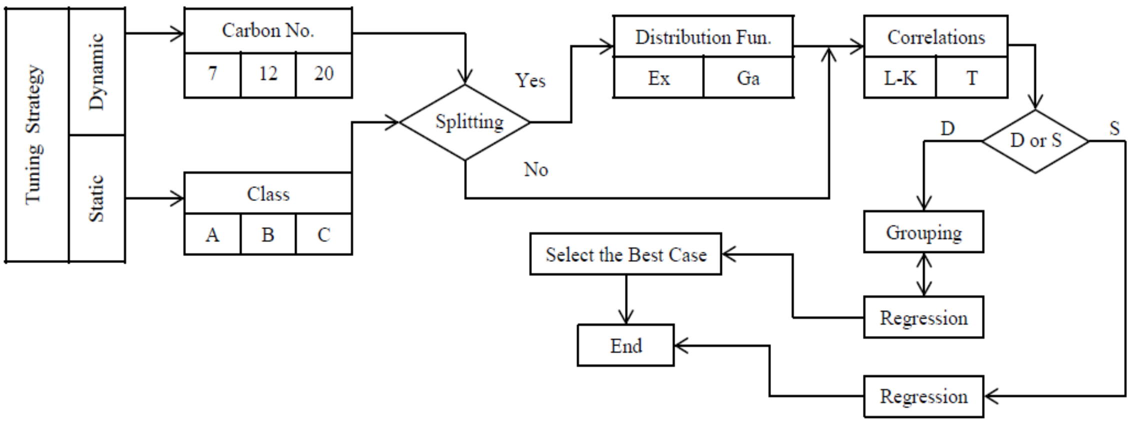

Figure 2
A schematic of characterization and tuning approach proposed for this study (Legends: Ex: exponential distribution function; Ga: Gamma distribution function; D: dynamic tuning; S: static tuning; L-K: Lee-Kesler's correlation; T: Twu's correlation).

4. Results and discussion

The proposed methodology described in the previous section was applied to three representative gas condensate samples having a valid measured PVT data. Based on this methodology, a sensitivity analysis was carried out on samples by varying some considerable variables such as the type of strategies, distribution functions, empirical correlations, and grouping method on EOS tuning. The abbreviations for each tuning path were described previously. Figure 3 shows the effect of all variables on average absolute deviation of P^{dew} predictions for sample W_1 by tuned EOS in a dynamic approach. By setting the maximum allowable AAD% for P^{dew} prediction equal to 1%, the simulation paths resulting in an AAD% ≤ 1% may be regarded as acceptable.

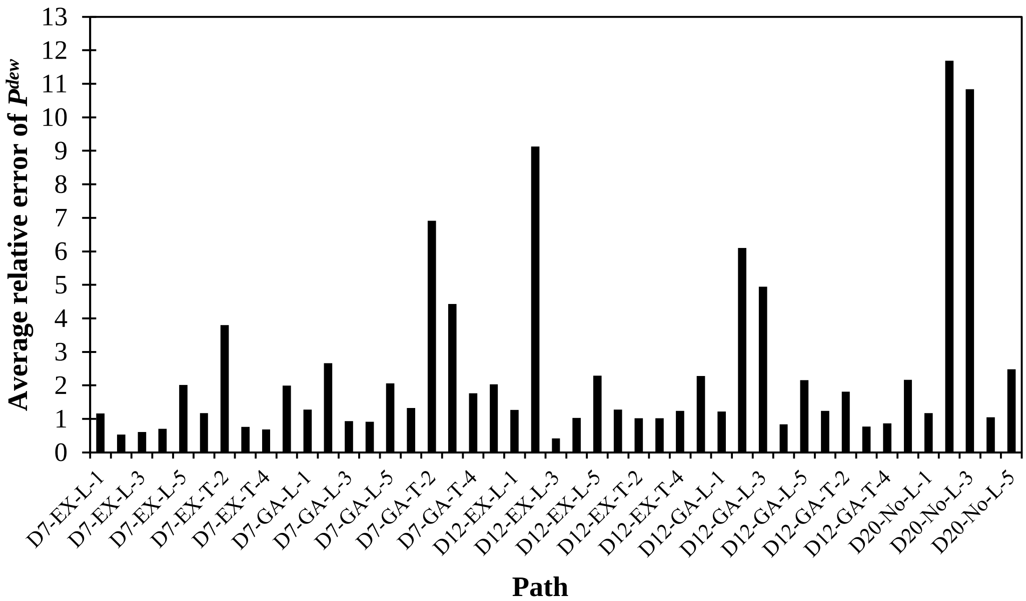

Figure 3
Average absolute deviation of P^{dew} predictions using tuned EOS for sample W_1 in the dynamic strategy.

Similar sensitivity analysis was made on other properties by setting a maximum allowable deviation for each sub-objective function. For example, Figures 4 and 5 show the effect of all the parameters on average absolute deviation of cumulative produce moles (CPM) and liquid drop-out predictions for the same sample in the dynamic approach respectively.

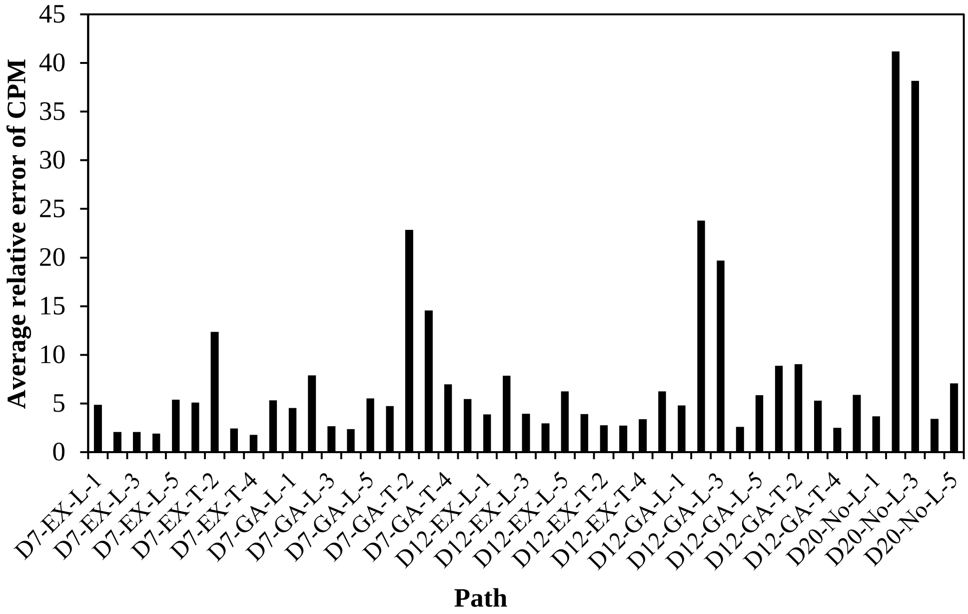

Figure 4
Average absolute deviation of CPM predictions using tuned EOS for sample W_1 in the dynamic strategy.

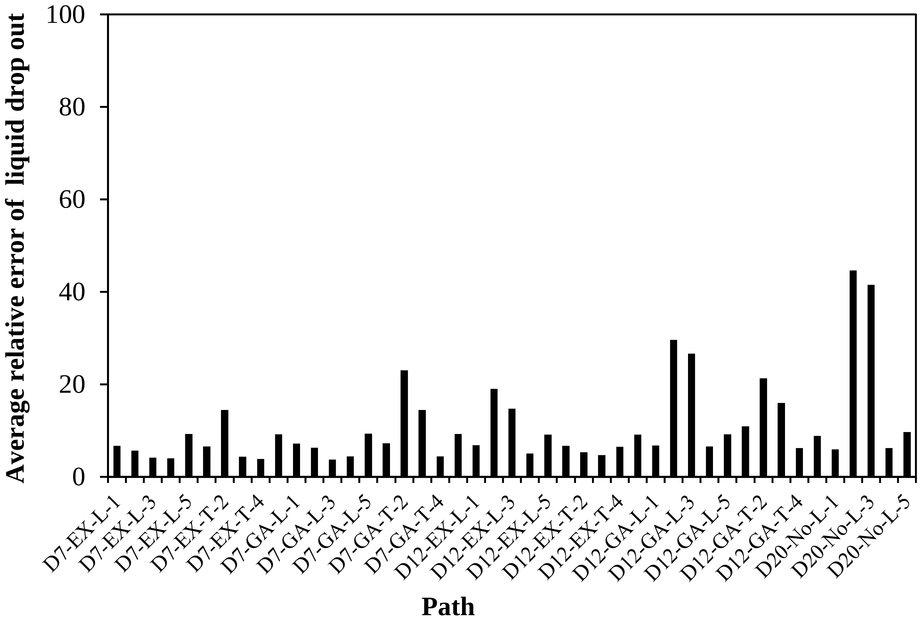

Figure 5
Average absolute deviation of liquid drop out predictions using tuned EOS for sample W_1 in the dynamic strategy.

The maximum allowable tolerance was set to 5% and 20% for these properties; it was also set on 2% and 3% for oil relative volume and gas compressibility factor respectively. If the accuracy of the predicted property by a specific "path" falls within the defined tolerance, the path will be assigned

“1”; otherwise, it will be assigned “0” to indicate that selected grouping and tuning “path” fails to predict the property correctly. The proposed “path” would succeed if only predictions fall within the acceptable range for all the five properties.

Table 4 summarizes the results of the EOS tuning sensitivity analysis of sample W_1. According to this table, there are eight acceptable “paths” for efficient fluid characterization and EOS tuning in this case. These paths include D7-EX-L-2, D7-EX-L-3, D7-EX-L-4, D7-EX-T-3, D7-EX-T-4, D7-GA-L-3, D7-GA-L-4, and D12-EX-L-3. All other possibilities fail to predict the fluid behavior correctly. Tables 5 and 6 summarize the results of samples W_2 and W_3, indicating that there are five and fourteen acceptable “paths” for these wells respectively.

Table 4

Results of the dynamic tuning strategy of sample W_1.

Path	P^{dew}	Relative volume	CPM	Liquid drop out	Z	Result
D7-EX-L-1	0	0	1	1	0	**0**
D7-EX-L-2	1	1	1	1	1	**1**
D7-EX-L-3	1	1	1	1	1	**1**
D7-EX-L-4	1	1	1	1	1	**1**
D7-EX-L-5	0	0	0	1	1	**0**
D7-EX-T-1	0	0	0	1	1	**0**
D7-EX-T-2	0	0	0	1	1	**0**
D7-EX-T-3	1	1	1	1	1	**1**
D7-EX-T-4	1	1	1	1	1	**1**
D7-EX-T-5	0	0	0	1	1	**0**
D7-GA-L-1	0	0	1	1	1	**0**
D7-GA-L-2	0	0	0	1	1	**0**
D7-GA-L-3	1	1	1	1	1	**1**
D7-GA-L-4	1	1	1	1	1	**1**
D7-GA-L-5	0	0	0	1	1	**0**
D7-GA-T-1	0	0	1	1	1	**0**
D7-GA-T-2	0	0	0	0	1	**0**
D7-GA-T-3	0	0	0	1	1	**0**
D7-GA-T-4	0	0	0	1	0	**0**
D7-GA-T-5	0	0	0	1	1	**0**
D12-EX-L-1	0	0	1	1	0	**0**
D12-EX-L-2	0	0	0	1	1	**0**
D12-EX-L-3	1	1	1	1	1	**1**
D12-EX-L-4	0	1	1	1	1	**0**
D12-EX-L-5	0	0	0	1	1	**0**
D12-EX-T-1	0	0	1	1	1	**0**
D12-EX-T-2	0	1	1	1	1	**0**
D12-EX-T-3	0	1	1	1	1	**0**

Path	P^{dew}	Relative volume	CPM	Liquid drop out	Z	Result
D12-EX-T-4	0	0	1	1	1	**0**
D12-EX-T-5	0	0	0	1	1	**0**
D12-GA-L-1	0	0	1	1	0	**0**
D12-GA-L-2	0	0	0	0	1	**0**
D12-GA-L-3	0	0	0	0	1	**0**
D12-GA-L-4	1	1	1	1	0	**0**
D12-GA-L-5	0	0	0	1	1	**0**
D12-GA-T-1	0	0	0	1	1	**0**
D12-GA-T-2	0	0	0	0	1	**0**
D12-GA-T-3	1	1	0	1	1	**0**
D12-GA-T-4	1	1	1	1	0	**0**
D12-GA-T-5	0	0	0	1	1	**0**
D20-No-L-1	0	1	1	1	0	**0**
D20-No-L-2	0	0	0	0	1	**0**
D20-No-L-3	0	0	0	0	1	**0**
D20-No-L-4	0	1	1	1	0	**0**
D20-No-L-5	0	0	0	1	1	**0**

Table 5
Results of the dynamic tuning strategy of sample W_2.

Path	P^{dew}	Relative volume	CPM	Liquid drop out	Z	Result
D7-EX-L-1	0	1	1	1	1	**0**
D7-EX-L-2	0	1	1	1	1	**0**
D7-EX-L-3	1	1	1	1	1	**1**
D7-EX-L-4	1	1	1	1	1	**1**
D7-EX-L-5	0	1	0	1	1	**0**
D7-EX-T-1	0	1	1	1	1	**0**
D7-EX-T-2	0	0	0	1	1	**0**
D7-EX-T-3	0	1	0	1	1	**0**
D7-EX-T-4	1	1	1	1	1	**1**
D7-EX-T-5	0	1	0	1	1	**0**
D7-GA-L-1	0	1	1	1	1	**0**
D7-GA-L-2	0	0	0	1	1	**0**
D7-GA-L-3	0	1	1	1	1	**0**
D7-GA-L-4	0	1	1	1	1	**0**
D7-GA-L-5	0	1	0	1	1	**0**
D7-GA-T-1	0	1	1	1	1	**0**
D7-GA-T-2	0	0	0	0	1	**0**
D7-GA-T-3	0	0	0	1	1	**0**

Path	P^{dew}	Relative volume	CPM	Liquid drop out	Z	Result
D7-GA-T-4	0	1	1	1	1	**0**
D7-GA-T-5	0	1	0	1	1	**0**
D12-EX-L-1	0	1	1	1	1	**0**
D12-EX-L-2	0	1	0	1	1	**0**
D12-EX-L-3	1	1	1	1	1	**1**
D12-EX-L-4	0	1	1	1	1	**0**
D12-EX-L-5	0	1	0	1	1	**0**
D12-EX-T-1	0	1	1	1	1	**0**
D12-EX-T-2	0	1	1	1	1	**0**
D12-EX-T-3	0	1	1	1	1	**0**
D12-EX-T-4	0	1	1	1	1	**0**
D12-EX-T-5	0	0	0	1	1	**0**
D12-GA-L-1	0	1	1	1	0	**0**
D12-GA-L-2	0	0	0	0	1	**0**
D12-GA-L-3	0	0	0	0	1	**0**
D12-GA-L-4	1	1	1	1	0	**0**
D12-GA-L-5	0	1	0	1	1	**0**
D12-GA-T-1	0	1	1	1	0	**0**
D12-GA-T-2	0	1	0	1	1	**0**
D12-GA-T-3	1	1	1	1	1	**1**
D12-GA-T-4	0	1	1	1	1	**0**
D12-GA-T-5	0	1	0	1	1	**0**
D20-No-L-1	0	1	1	1	0	**0**
D20-No-L-2	0	0	0	0	1	**0**
D20-No-L-3	0	0	0	0	1	**0**
D20-No-L-4	0	1	1	1	0	**0**
D20-No-L-5	0	1	0	1	1	**0**

Table 6

Results of the dynamic tuning strategy of sample W_3.

Path	P^{dew}	Relative volume	CPM	Liquid drop out	Z	Result
D7-EX-L-1	1	1	1	1	1	**1**
D7-EX-L-2	0	1	1	1	1	**0**
D7-EX-L-3	1	1	1	1	1	**1**
D7-EX-L-4	1	1	1	1	1	**1**
D7-EX-L-5	0	1	1	1	1	**0**
D7-EX-T-1	1	0	1	1	1	**0**
D7-EX-T-2	0	0	0	1	1	**0**
D7-EX-T-3	0	1	0	1	1	**0**

Path	P^{dew}	Relative volume	CPM	Liquid drop out	Z	Result
D7-EX-T-4	1	1	1	1	1	**1**
D7-EX-T-5	0	1	0	1	1	**0**
D7-GA-L-1	0	1	1	1	1	**0**
D7-GA-L-2	0	0	0	1	1	**0**
D7-GA-L-3	1	1	1	1	1	**1**
D7-GA-L-4	1	1	1	1	1	**1**
D7-GA-L-5	0	0	1	1	1	**0**
D7-GA-T-1	0	0	1	1	1	**0**
D7-GA-T-2	0	0	0	0	1	**0**
D7-GA-T-3	0	0	0	1	1	**0**
D7-GA-T-4	1	1	1	1	1	**1**
D7-GA-T-5	0	0	1	1	1	**0**
D12-EX-L-1	1	0	1	1	0	**0**
D12-EX-L-2	1	1	1	1	1	**1**
D12-EX-L-3	1	1	1	1	1	**1**
D12-EX-L-4	1	1	1	1	1	**1**
D12-EX-L-5	0	0	1	1	1	**0**
D12-EX-T-1	1	0	1	1	1	**0**
D12-EX-T-2	0	0	1	1	1	**0**
D12-EX-T-3	1	1	1	1	1	**1**
D12-EX-T-4	1	1	1	1	1	**1**
D12-EX-T-5	0	0	1	1	1	**0**
D12-GA-L-1	1	0	1	1	0	**0**
D12-GA-L-2	0	0	0	1	1	**0**
D12-GA-L-3	0	0	0	1	1	**0**
D12-GA-L-4	1	1	1	1	0	**0**
D12-GA-L-5	0	0	1	1	1	**0**
D12-GA-T-1	1	0	1	1	0	**0**
D12-GA-T-2	1	1	0	1	1	**0**
D12-GA-T-3	1	1	1	1	1	**1**
D12-GA-T-4	1	1	1	1	1	**1**
D12-GA-T-5	0	0	1	1	1	**0**
D20-No-L-1	1	1	1	1	0	**0**
D20-No-L-2	0	0	0	0	1	**0**
D20-No-L-3	0	0	0	1	1	**0**
D20-No-L-4	1	1	1	1	0	**0**
D20-No-L-5	0	0	1	1	1	**0**

Figure 6 shows the frequency plot for SCN, distribution function, empirical correlations, and grouping step which describe the most accurate paths in the dynamic tuning strategy. Based on this sensitivity analysis, a combination of SCN= 7 for plus fraction, exponential distribution function, Lee-Kesler's (Lee and Kesler, 1975) correlation for estimating critical properties, and the third or the fourth step in grouping (Whitson and Brule, 2000) would result in the best EOS tuning and fluid property prediction. Also, this figure shows that increasing the SCN of plus fraction and grouping steps does not necessarily result in better outputs with higher accuracy.

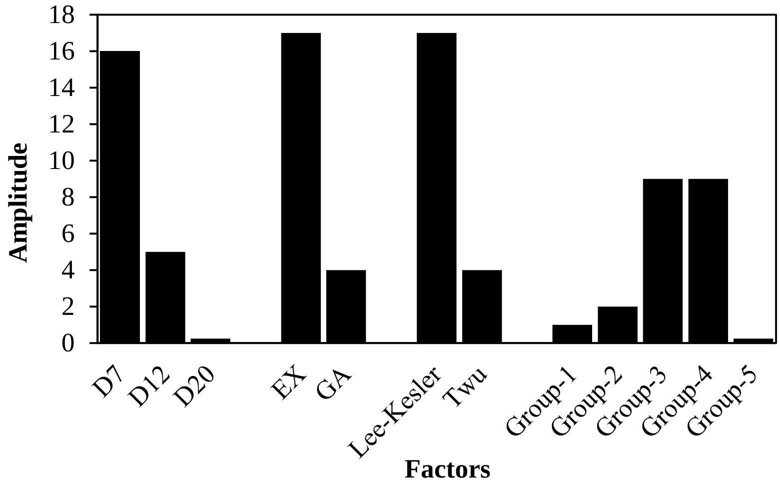

Figure 6

Frequency plot for SCN, distribution function, empirical correlations, and grouping step of the most accurate paths in the dynamic strategy.

The results of employing the static tuning strategy are summarized in Tables 7-9 for wells W_1, W_2, and W_3 respectively. Moreover, a typical phase envelop checking is illustrated in Figure 7. As it can be seen, the phase envelops before and after characterization-tuning procedure are the same. This approach is simpler to use as the fluid composition is fixed and there are less possible combinations to study. Comparing the static and dynamic tuning strategies suggest that the dynamic strategy offer better results if there is no constraint on the fluid composition. In the cases where fluid composition is to be set a priori, the static strategy may be applied. Furthermore, the increased number of fluid characterization and EOS tuning steps is associated with the larger number of optimization parameters for minimizing the objective function. As a result, the overall number of computation steps is higher in the dynamic tuning strategy compared to the static strategy.

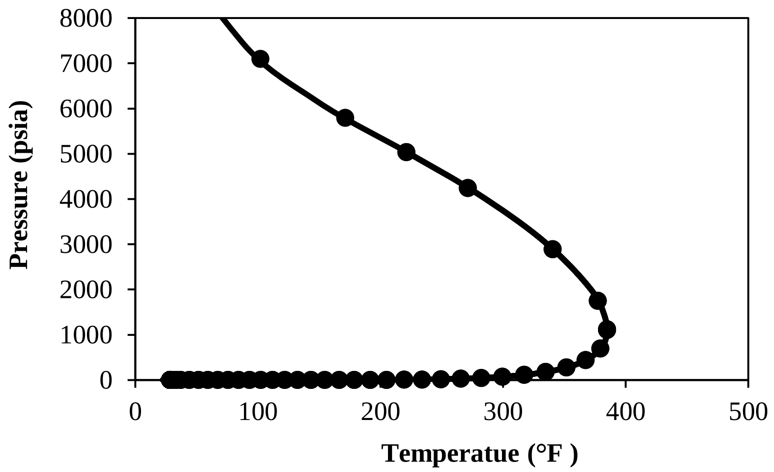

Figure 7

Phase envelops for well W_1 (Path: B-Ga-T) before (-) and after (•) characterization-tuning procedure.

Table 7
Results of the static tuning strategy of well W_1.

Path	P^{dew}	Relative volume	CPM	Liquid drop out	Z	Result
A-No-L	0	0	1	1	1	0
A-No-T	0	0	0	1	1	0
B-EX-L	0	0	1	1	1	0
B-EX-T	0	0	0	1	1	0
B-GA-L	0	0	1	1	1	0
B-GA-T	1	1	1	1	1	1
C-No-L	0	0	1	1	1	0
C-No-T	0	0	1	1	1	0

Table 8
Results of the static tuning strategy of well W_2.

Path	P^{dew}	Relative volume	CPM	Liquid drop out	Z	Result
A-No-L	0	0	0	1	1	0
A-No-T	1	1	1	1	1	1
B-EX-L	0	0	1	1	1	0
B-EX-T	0	0	1	1	1	0
B-GA-L	0	0	1	1	1	0
B-GA-T	0	0	1	1	1	0
C-No-L	0	0	1	1	1	0
C-No-T	0	0	1	1	1	0

Table 9
Results of the static tuning strategy of well W_3.

Path	P^{dew}	Relative volume	CPM	Liquid drop out	Z	Result
A-No-L	0	0	0	1	1	0
A-No-T	0	0	1	1	1	0
B-EX-L	0	0	1	1	1	0
B-EX-T	1	1	1	1	1	1
B-GA-L	1	1	1	1	1	1
B-GA-T	1	1	1	1	1	1
C-No-L	0	1	1	1	1	0
C-No-T	0	0	1	1	1	0

5. Conclusions

The proposed algorithm showed that both fluid characterization and EOS tuning have a significant impact on the fluid phase behavior model, and when they are used simultaneously, the most acceptable results, or more precisely paths, can be achieved. When there is flexibility in final grouping of the fluid components, the dynamic approach is more effective than the other approaches. Since the dynamic approach examines all the factors and available levels on the objective function, achieving the global minimum of the non-linear objective function is more probable compared to the static approach. The application of the proposed integrated fluid characterization and EOS tuning algorithm to the selected gas condensate samples showed that the SCN= 7 for plus fraction combined with exponential distribution function, Lee-Kesler's correlation, and the third- or fourth-step of the seven-step Whitson's grouping method can increase the accuracy of fluid model for the studied field. According to the proposed algorithm, the static approach may be successfully applied to systems with an interest in the special combination of component grouping such as the compositional gradient of certain components and wax or asphaltene deposition. This technique can also give accurate results with a local minimum of the objective function. The static approach requires less processing time as it has less computation steps compared to the dynamic technique.

Nomenclatures

CCE	: Constant composition expansion
CGR	: Condensate gas ratio
CPM	: Cumulative produce moles (moles)
CVD	: Constant volume depletion
D	: Dynamic
DST	: Drill-stem test
EOS	: Equation of state
Exp.	: Exponential function
Ga	: Gamma function
MW	: Molecular weight (gr/mole)
P	: Pressure (psia)
RLD	: Relative liquid drop-out
RV	: Relative volume
S	: Static
SCN	: Single carbon number
T	: Temperature (°F)
Greek Letters	
κ	: Dimension less parameter in Equation 7
ω	: Acentric factor
Ω_a, Ω_b	: Adjustable parameters in equations 4 and 5
Superscripts	
cal	: Calculated
dew	: Dew point
exp	: Experimental
Subscript	
c	: Critical

References

Aguilar Zurita, R. A. and McCain Jr., W. D., An Efficient Tuning Strategy to Calibrate Cubic EOS for Compositional Simulation, SPE 77382, 2002.

Ahmed, T., Equations of State and PVT Analysis: Applications for Improved Reservoir Modeling. 1st Edition, Gulf Publishing, Houston, Texas, 2007.

Ahmed, T., Hydrocarbon Phase Behavior, Gulf Publishing Company, 1989.

Al-Meshari, A. A., Aquilar-Zarita, R. A., and McCain Jr., W. D., Tuning an Equation of State- the Critical Importance of Correctly Grouping Composition into Pseudo-components, SPE Annual Technical Conference and Exhibition, Dallas, Texas: Society of Petroleum Engineers, 2005.

Danesh A., PVT and Phase Behavior of Petroleum Reservoir Fluids, 1st ed., Amsterdam: Elsevier, 1998.

Edgar, T. F., Optimization of Chemical Processes: McGraw-Hill, 2nd ed., 2001.

Fevang, O., Gas-condensate Flow Behavior and Sampling, Norway: University of Trondheim, 1995.

Hoffman, A. E., Crump, J. S., and Hocott, C. R., Equilibrium Constants for a Gas Condensate System, Trans AIME, Vol. 198, p.1-10, 1953.

Hosein, R. and Dawe, R. A., Tuning of the Peng-Robinson Equation of State for Gas Condensate Simulation Studies, SPETT 2012 Energy Conference and Exhibition. Port-of-Spain, Trinidad: Society of Petroleum Engineers, 2012.

Hosein, R. and Jagai, T., Optimizing the Number of Components in Tuning the Peng-Robinson Equation-of-state for Trinidad's Gas Condensates, SPE Latin American and Caribbean Petroleum Engineering Conference. Port-of-Spain, Trinidad and Tobago: Society of Petroleum Engineers, 2003.

Imo-Jack, O., PVT Characterization of a Gas condensate Reservoir and Investigation of Factors Affecting Deliverability, Nigeria Annual International Conference and Exhibition, Tinapa-Calabar, Nigeria: Society of Petroleum Engineers, 2010.

Kool H., Azari M., Soleiman, M. Y., Proett, M. A., Irani, C. A., and Dybdahl, B., Testing of Gas Condensate Reservoirs-sampling, Test Design and Analysis, SPE Asia Pacific Oil and Gas Conference and Exhibition, Jakarta, Indonesia: Society of Petroleum Engineers, 2001.

Lee, B. I. and Kesler, M. G., A Generalized Thermodynamic Correlation Based on Three-parameter Corresponding States, AIChE Journal, Vol. 21, p. 510-527, 1975.

McCain Jr., W. B. and Alexander, R. A., Sampling Gas Condensate Wells, SPE Asia Pacific Oil and Gas Conference, Jakarta, Indonesia: Society of Petroleum Engineers, 1992.

Mehrabian, A. and Crespo, F., A New Multi-sample EOS Model for the Gas Condensate Phase Behavior Analysis, Oil and Gas Science and Technology, Vol. 66, p. 1025-1033, 2011.

Merrill, R. C., Hartman, K. J., and Creek J. L., A Comparison of Equation of State Tuning Methods, SPE Annual Technical Conference and Exhibition, New Orleans, Louisiana, USA: Society of Petroleum Engineers, 1994.

Moshfeghian, M., Maddox, R. N., and Johanson, A. H., Application of Exponential Decay Distribution of C_{6+} Cut for Lean Natural Gas Phase Envelope, Journal of Chemical Engineering of Japan, Vol. 39, p. 375-382, 2006.

Nasrifar, K. and Moshfeghian, M., Vapor–liquid Equilibria of LNG and Gas Condensate Mixtures by the Nasrifar–Moshfeghian Equation of State, Fluid Phase Equilibria, Vol. 190, p. 73-88, 2002.

Nasrifar, K., Bolland, O., and Moshfeghian, M., Predicting Natural Gas Dew Points from 15 Equations of States, Energy and Fuels, Vol. 19, p. 561-72, 2005.

Nazarzadeh, M. and Moshfeghian, M., New volume Translated PR Equation of State for Pure Compounds and Gas Condensate Systems, Fluid Phase Equilibria, Vol. 337, p. 214-23, 2013.

Osfouri, S., Azin, R., Kiani Zakheradi, M., and Gerami, S., A Unified Approach for Quality Control of Drilled Stem Test (DST) and PVT Data, Gas Processing Journal, Vol. 2, No. 1, p. 40-50, 2014.

Patel, N. C. and Teja, A. S., A New Equation of State for Fluids and Fluid Mixtures, Chemical Engineering Science, Vol. 37, p. 463-73, 1982.

Pedersen, K. S., Blilie, A. L., and Meisingset, K. K., PVT Calculations on Petroleum Reservoir Fluids Using Measured and Estimated Compositional Data for the Plus Fraction, Industrial and Engineering Chemical Research, Vol. 31, p. 1378-1384, 1992.

Pedersen, K. S., Thomassen P., and Fredenslund, A., on the Danger of “Tuning” Equation of State Parameters, SPE 14487: Society of Petroleum Engineering, 1985.

Pedersen, K. S., Thomassen, P., and Fredenslund, A., Characterization of Gas Condensate Mixtures, Presented in Chorn L.G. and Mansoori G.A.: C_{7+} Fraction Characterization, Taylor & Francis New York Inc., New York, 1989.

Peng, D. and Robinson, D., A New Two Constant Equation of State, Industrial Engineering and Chemistry Fundamentals, Vol. 15, p. 59-64, 1976.

Schebetov, A., Rimoldi, A., and Piana, M., Quality Check of Gas Condensate PVT Studies and EOS Modelling Under Input Data Uncertainty, SPE Russian Oil and Gas Conference and Exhibition, Moscow, Russia: Society of Petroleum Engineers, 2010.

Shariati, A., Peters, C. J., and Moshfeghian, M., Further Evaluation of the Shariati-Peters-Moshfeghian C_{7+} Characterization Method, Fluid Phase Equilibria, Vol. 179, p. 23-41, 2001.

Soave, G., Equilibrium Constants from a Modified Redlich-Kwong Equation of State, Chemical Engineering and Science, Vol. 27, p. 1197-1203, 1972.

Thomas, F. B., Shtepani, E., Imer, D., and Bennion, D. B., Representing Reservoir Oil Using Recombination Techniques, Journal of Canadian Petroleum Technology, Vol. 46, p. 6-12, 2007.

Twu, C. H., An Internally Consistent Correlation for Predicting the Critical Properties and Molecular Weights of Petroleum and Coal-tar Liquids, Fluid Phase Equilibria, Vol. 16, p. 137-150, 1984.

Wei, Y. S. and Sadus, R. J., Equations of State for the Calculation of Fluid-phase Equilibria, AIChE Journal, Vol. 46, p. 169-96, 2000.

Whitson, C. H., Anderson, T. F., and Soreide, I., Application of the Gamma Distribution Model to Molecular Weight and Boiling Point Data for Petroleum Fractions, Chemical Engineering Communications, Vol. 96, p. 259-278, 1990.

Whitson, C. H., Characterizing Hydrocarbon Plus Fraction, Society of Petroleum Engineers Journal, Vol. 23, p. 683-94, 1983.

Whitson, C.H. and Brule, M. R. PHASE behavior, SPE Monograph, 2000.

Yarborough, L., Application of a Generalized Equation of State to Petroleum Reservoir Fluids, Equations of State in Engineering and Research, Advances in Chemistry, American Chemical Society, Vol. 182, Chapter 21, p. 385-439,1979.

Appendix

Table A1

CVD experimental data of three representative samples.

Well name	Pressure (psia)	Retrograde liquid deposit (Vol.% at P_d)	Cumulative produced fluid (mol.%)	Z
	4695	0	0	0.98
	4415	0.19	4.17	0.964
	3715	1.04	15.94	0.925
W_1	2915	1.96	31.82	0.895
	2215	2.46	47.47	0.887
	1415	2.62	66.51	0.903
	822	2.49	81.68	0.933
	4950	0	0	1.001
	4615	0.21	4.59	0.981
	3815	1.08	17.14	0.933
W_2	3015	2.01	32.16	0.899
	2215	2.56	49.32	0.889
	1415	2.68	67.69	0.903
	788	2.6	80.47	0.932
	4682	0	0	0.985
	4315	0.27	5.54	0.96
	3615	1.04	17.64	0.92
W_3	2915	1.81	31.7	0.895
	2215	2.3	47.39	0.889
	1415	2.42	66.46	0.907
	880	2.34	80.34	0.929

Table A2
CCE experimental data of three representative samples.

W1				W2				W3			
P (psia)	RV	RLD	Z	P (psia)	RV	RLD	Z	P (psia)	RV	RLD	Z
8015	0.755		1.263	8015	0.781		1.266	8015	0.748		1.261
7515	0.775		1.216	7015	0.827		1.174	7515	0.768		1.215
7015	0.8		1.171	6015	0.894		1.088	7015	0.793		1.17
6515	0.83		1.128	5515	0.939		1.047	6515	0.823		1.127
6015	0.865		1.086	5315	0.959		1.031	6015	0.859		1.087
5515	0.909		1.046	5215	0.97		1.023	5515	0.904		1.048
5215	0.939		1.022	5104	0.981		1.015	4994	0.958		1.01
5094	0.952		1.012	5015	0.992		1.006	4915	0.97		1.003
5015	0.961		1.006	4965	0.998		1.002	4815	0.982		0.995
4915	0.973		0.998	4950	1	0	1.001	4765	0.989		0.991
4815	0.985		0.99	4925	1.003	0.01		4715	0.996		0.987
4765	0.991		0.986	4905	1.006	0.03		4682	1	0	0.985
4715	0.997		0.982	4885	1.008	0.04		4655	1.005	0.02	
4695	1	0	0.98	4865	1.011	0.05		4635	1.008	0.03	
4675	1.003	0.01		4845	1.014	0.07		4615	1.011	0.05	
4655	1.006	0.02		4815	1.018	0.09		4595	1.013	0.06	
4635	1.009	0.04		4765	1.025	0.12		4565	1.018	0.09	
4615	1.012	0.05		4715	1.032	0.16		4515	1.026	0.13	
4595	1.014	0.07		4615	1.047	0.25		4465	1.034	0.17	
4565	1.019	0.09		4515	1.063	0.34		4415	1.042	0.21	
4515	1.026	0.13		4315	1.098	0.55		4315	1.059	0.31	
4465	1.034	0.17		4115	1.138	0.8		4215	1.078	0.41	
4415	1.042	0.22		3815	1.207	1.2		4015	1.118	0.64	
4315	1.059	0.31		3515	1.29	1.63		3815	1.163	0.89	
4215	1.078	0.42		3115	1.432	2.19		3515	1.245	1.28	
4015	1.118	0.66		2715	1.623	2.69		3215	1.348	1.68	
3815	1.165	0.93		2215	1.97	3.14		2815	1.525	2.19	
3515	1.248	1.36		1815	2.408	3.35		2415	1.77	2.61	
3215	1.349	1.81		1615	2.717	3.42		1915	2.24	2.98	
2815	1.526	2.36		1415	3.128	3.44		1715	2.512	3.08	
2415	1.774	2.79		1257	3.539	3.4		1515	2.851	3.12	
1915	2.249	3.1						1279	3.407	3.08	
1715	2.526	3.16									
1515	2.878	3.19									
1295	3.429	3.18									